Inorg. Chem. **2008**, *47*, 2274−2279

Theoretical Study on $(Al_2O_3)_n$ (n = 1–10 and 30) Fullerenes and H_2 Adsorption Properties

Jiao Sun,[†] Wen-Cai Lu,[*,†,‡] Wei Zhang,[†] Li-Zhen Zhao,[†] Ze-Sheng Li,[†] and Chia-Chung Sun[†]

State Key Laboratory of Theoretical and Computational Chemistry, Institute of Theoretical Chemistry, Jilin University, Changchun, Jilin 130021, PR China, and Department of Physics, Qingdao University, Qingdao, Shandong 266071, PR China

Received June 10, 2007

The structures and stabilities of $(Al_2O_3)_n$ (n = 1–10 and 30) clusters were studied by means of first principles calculations. The calculated results reveal that the global minima of small $(Al_2O_3)_n$ (n = 1–5) clusters are cage structures with high symmetries, in which Al and O atoms are three- and two-coordinated, respectively, and are linked to neighbors via single bonds. Beyond $(Al_2O_3)_5$, we calculated both cage and cage-dimer structures for $(Al_2O_3)_n$ (n = 6–10), and the results show that, at this size range, cage-dimer structures are more stable than cage structures. Furthermore, an onion-like motif for $(Al_2O_3)_{10}$ was studied, and it is interesting to find that, at this size, the onion structure is more favorable than cage and cage-dimer structures. For large clusters, a shell structure of $Al_{60}O_{90}$ is suggested. Electronic properties and calculations on hydrogen adsorption of these aluminum oxide structures are reported, and we discuss their possible use as hydrogen storage materials.

Introduction

Metal aluminum and its compounds play an important role in various fields such as synthesis, catalysis, alloys, etc., and especially, aluminum leads to a new area in the synthesis of materials. In the studies of aluminum combustion, it has been found via observing alumina aerosol that aluminum droplets have a global combustion behavior, which was inspired by both fundamental interest[1,2] and possible applications.[3] In particular, the combustion of metal powder can be an effective way to synthesize semiconductor and ceramic oxide nanoparticles.[3] In a high-speed shadow microphotography image of a burning Al droplet, one can see a smoke tail (or aerogelation zone), where the long chain-like aggregates of tens of microns in length are formed.[4] The alumina nanoparticles form aggregates of about 1 μm composed of primary particles with a diameter of a few tens of nanometers. Recently, Peng et al. synthesized Al_2O_3 microtubes by applying atomic layer deposition on electrospun polymer fibers, in which case Al_2O_3 film is grown layer-by-layer on the substrate and its smallest thickness can be controlled to about 14 nm.[5] Studies on the properties and applications of these novel nanostructures of aluminum oxides will be expected.

After the discovery of the C_{60} molecule by Kroto et al.[6,7] in 1985, the search for the possible existence of fullerenes and nanotubes based on elements other than carbon has received much attention. The group III nitrides have been the subject of extensive investigation in this area, especially after pure BN nanotubes were synthesized.[8] AlN fullerenes

* E-mail: wencailu@jlu.edu.cn.
† Jilin University.
‡ Qingdao University.

(1) Dreizin, E. L. *Combust. Flame* **1999**, *116*, 323.
(2) Price, E. W.; Sigman, R. K. Solid Progress Chemistry, Combustion, and Motor Interior Ballistics. In *Progress in Astronautics and Aeronautics*Yang, V., Brill, T. B., Ren, W.-Z., Eds.; AIAA: Reston, VA, 2000; Chapter 2.18, Vol. 185, pp 663–687.
(3) Zolotko, A. N.; Vovchuk, Ya. I.; Poletaev, N. I.; Florko, A. V.; Altman, I. S. *Combust. Explos. Shock Waves* **1996**, *32*, 24.
(4) Karasev, V. V.; Onischuk, A. A.; Glotov, O. G.; Baklanov, A. M.; Maryasov, A. G.; Zarko, V. E.; Panfilov, V. N.; Levykin, A. I.; Sabelfeld, K. K. *Combust. Flame* **2004**, *138*, 40.
(5) Peng, Q.; Sun, X.-Y.; Spagnola, J. C.; Hyde, G. K.; Spontak, R. J.; Parsons, G. N. *Nano Lett.* **2007**, *7*, 719.
(6) Dresselhaus, M. S.; Dresselhaus, G.; Eklunf, P. C. *Science of Fullerenes and Carbon Nanotubes*, Academic Press: New York, 1996.
(7) Kroto, H. W.; Heath, J. R.; O'Brien, S. C.; Curl, R. F.; Smalley, R. E. *Nature* **1985**, *318*, 162.
(8) Chopra, N. G.; Luyren, R. J.; Cherry, K.; Crespi, V. H.; Cohen, M. L.; Louis, S. G.; Zettl, A. *Science* **1995**, *269*, 966.
(9) Chen, X.; Ma, J.; Hu, Z.; Wu, Q.; Chen, Y. *J. Am. Chem. Soc.* **2005**, *127*, 7982.
(10) Zhang, D.; Zhang, R. Q. *J. Mater. Chem.* **2005**, *15*, 3034.
(11) Zhao, M. W.; Xia, Y. Y.; Liu, X. D.; Tan, Z. Y.; Huang, B. D.; Song, C.; Mei, L. M. *J. Phys. Chem. B* **2006**, *110*, 8764.
(12) Zope, R. R.; Dunlap, B. I. *Phys. Rev. B* **2005**, *72*, 045439.
(13) Balasubramanian, C.; Godbole, V. P.; Rohatgi, V. K.; Das, A. K.; Bhoraskar, S. V. *Nanotechnology* **2004**, *15*, 370.

10.1021/ic7011364 CCC: $40.75
Published on Web 02/27/2008

have similar structures as predicted and observed for BN cages. A lot of theoretical[9–12] and correlative experimental[13] studies propose the possible existence of AlN fullerenes, although they have not yet been found experimentally. Spanó et al. used a simulated annealing method to obtain the global minima of $(ZnS)_n$ with n ranging from 10 to 60.[14,15] The clusters have "bubble"-like polyhedral structures, while $(ZnS)_{60}$ is an onion-like structure with one small cluster enclosed inside a bigger one.

Well then, does global combustion produce fullerene structures? Although oxidation of aluminum has received more attention from theoretical and experimental studies, the global combustion of Al, especially the more detailed investigation about structures and properties of the combustion products, is still lacking. So far, only Onischuk et al. predicted, in a simple way, the possible existence of the $(Al_2O_3)_{1-5}$ and $Al_{20}O_{30}$ fullerene-like structures.[16] A systematic study on $(Al_2O_3)_n$ is required and will provide useful information for experiments.

In the present work, we report our studies on the geometries, electronic structures, and stabilities of $(Al_2O_3)_n$ (n = 1–10 and 30) clusters. The clusters at nanoscale may possess special chemical or physical properties. The possible use of $(Al_2O_3)_n$ as a hydrogen storage material, due to their cage structures, is also discussed. As it is well-known, hydrogen is an important energy carrier for sustainable energy consumption with a reduced impact on the environment, and searching for efficient hydrogen storage material is now a hot point in materials research.

Computational Methods

All of the calculations have been carried out using the GAUSSIAN 03 package.[17] The geometries were fully optimized at the B3LYP[18]/6-311+G(3df,2p) level for small-sized clusters $(Al_2O_3)_{1-5}$. For medium-sized $(Al_2O_3)_{6-10}$, the B3LYP/6-31G(d,p) level was used to optimize their single- and double-cage structures. For the larger fullerene $Al_{60}O_{90}$, the calculations were performed at the B3LYP/6-31G(d,p)//B3LYP/6-31G(d). Vibrational frequencies were also calculated, and structures with only real frequencies are confirmed as minima. Natural population analyses (NPA) and natural bond orbital (NBO) analyses were performed using the NBO[19] program as implemented in the GAUSSIAN 98 program.

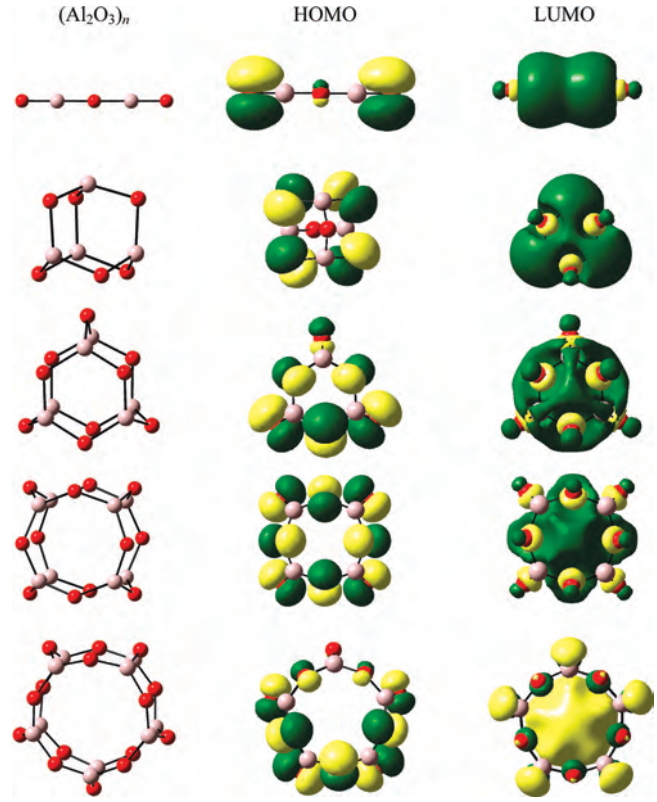

Figure 1. Optimized geometries and their HOMOs and LUMOs (isodensity value is 0.02) for $(Al_2O_3)_{1-5}$ clusters at the B3LYP/6-31G(d,p) level.

Results and Discussion

A. $(Al_2O_3)_n$ (n = 1–10 and 30) Clusters. For $(Al_2O_3)_{1-5}$, a mass of possible initial configurations was considered, and we report only a selection of the most stable configurations. Beyond this size, the $(Al_2O_3)_{6-10}$ cage and cage-dimer structures were studied. In this work, a larger fullerene structure was constructed based on the foregoing smaller one; for example, inserting a linear Al_2O_3 into one ring in $(Al_2O_3)_n$ can make the ring separate into two rings, leading to an $(Al_2O_3)_{n+1}$ fullerene. For $(Al_2O_3)_{6-10}$ cage-dimer structures, as many as possible linkages between two cages were considered.

The $(Al_2O_3)_n$ (n = 1–10) cluster structures are shown in Figures 1−4. The corresponding geometrical parameters are given in Table 1. The lowest-energy structures of $(Al_2O_3)_{2-5}$ clusters are cage fullerenes with high symmetries. The fullerenes consist of 6-, 8-, or 10-membered rings with saturated valence states of Al and O atoms on the surfaces. The Al−O−Al angles increase along with larger fullerene size. For all Al_2O_3 cages, the lengths of the Al−O bond are at a narrow range of 1.70−1.71 Å, which are smaller than those in general aluminum oxides clusters and bulk Al_2O_3. Note that the presented $(Al_2O_3)_n$ (n = 2–5) cages correspond

(14) Spano, E.; Hamad, S.; Catlow, C. R. A. *J. Phys. Chem. B* **2003**, *107*, 10337.
(15) Spano, E.; Hamad, S.; Catlow, C. R. A. *Chem. Commun.* **2004**, *4*, 864.
(16) Onischuk, A. A.; Karasev, V. V.; Glotov, O. G.; Baklanov, A. M.; Chernyshev, A. V.; Zarko, V. E. *Abstracts of the European Aerosol Conference*, **2003**.
(17) Frisch, M. J.; Trucks, G. W.; Schlegel, H. B.; Scuseria, G. E.; Robb, M. A.; Cheeseman, J. R.; Zakrzewski, V. G.; Montgomery, J. A., Jr.; Stratmann, R. E.; Burant, J. C.; Dapprich, S.; Millam, J. M.; Daniels, A. D.; Kudin, K. N.; Strain, M. C.; Farkas, O.; Tomasi, J.; Barone, V.; Cossi, M.; Cammi, R.; Mennucci, B.; Pomelli, C.; Adamo, C.; Clifford, S.; Ochterski, J.; Petersson, G. A.; Ayala, P. Y.; Cui, Q.; Morokuma, K.; Malick, D. K.; Rabuck, A. D.; Raghavachari, K.; Foresman, J. B.; Cioslowski, J.; Ortiz, J. V.; Stefanov, B. B.; Liu, G.; Liashenko, A.; Piskorz, P.; Komaromi, I.; Gomperts, R.; Martin, R. L.; Fox, D. J.; Keith, T.; Al-Laham, M. A.; Peng, C. Y.; Nanayakkara, A.; Gonzalez, C.; Challacombe, M.; Gill, P. M. W.; Johnson, B. G.; Chen, W.; Wong, M. W.; Andres, J. L.; Head-Gordon, M.; Replogle, E. S.; Pople, J. A. *GAUSSIAN 03*, revision B. 03; Gaussian, Inc.: Pittsburgh, PA, 2003.
(18) (a) Becke, A. D. *J. Chem. Phys.* **1993**, *98*, 5648. (b) Lee, C.; Yang, W.; Parr, R. G. *Phys. Rev. B* **1988**, *37*, 785. (c) Mielich, B.; Savin, A.; Stoll, H.; Preuss, H. *Chem. Phys. Lett.* **1989**, *157*, 200.
(19) Bohmann, J. A.; Weinhold, F.; Farrar, T. C. *J. Chem. Phys.* **1997**, *107*, 1173(NBO3.0 is available in the Gaussian 03 program, but the more advanced NBO5.0 version be installed in Gaussian 98).

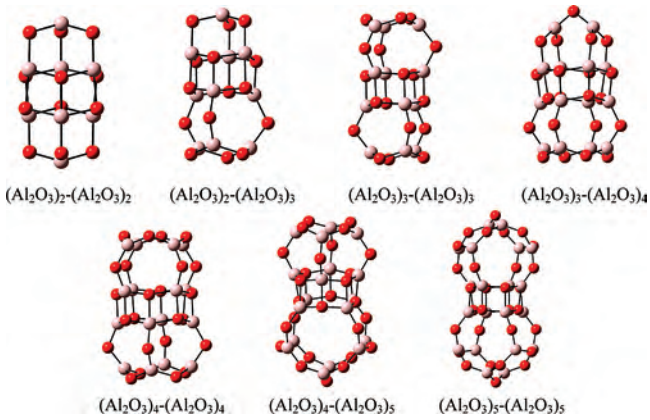

Figure 2. Optimized geometries for $(Al_2O_3)_{4-10}$ dimers at the B3LYP/6-31G(d,p) level.

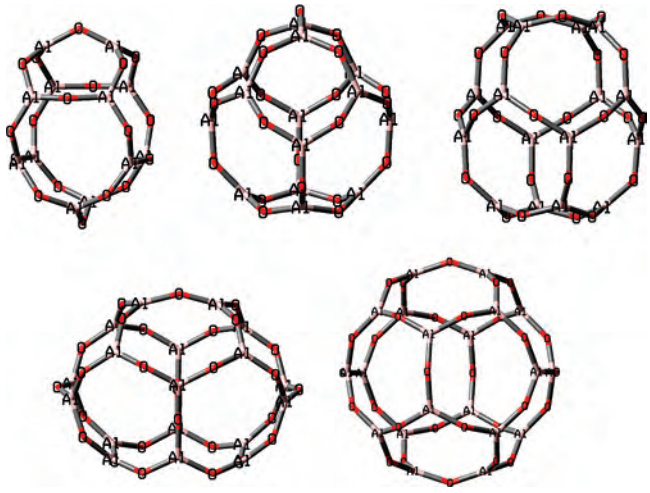

Figure 3. Optimized geometries for $(Al_2O_3)_{6-10}$ cages at the B3LYP/6-31G(d,p) level.

to global minimum structures, and after $n = 5$, we predict that the most stable structures are no longer cages.

It seems that size effect is important for cage-like structure stability due to strain energy. Owing to steric and size effects, large cages might be less stable. For $(Al_2O_3)_{6-10}$, we designed both cage and cage-dimer motifs (Figures 2 and 3), and the latter consists of two small cages from $(Al_2O_3)_{2-5}$. We have constructed many linkages between two cages which are liked by Al−O single bonds or AlO rings, and the presented structures correspond to the most favorable combinations we find. In the cage-dimer structures (Figure 2), the Al−O bonds linking two cages are around 1.9 Å, about 0.2 Å larger than those in cage structures. The calculated thermodynamic results show that for $(Al_2O_3)_{6-10}$ the cage-dimer structures are more stable than the cage structures. Thus, the $(Al_2O_3)_5$ cage is expected to be the largest cage as the global minimum. One may also wonder if $(Al_2O_3)_{6-10}$ clusters can have stable onion-like structures. For this reason, we constructed an $(Al_2O_3)_2@(Al_2O_3)_8$ isomer (Figure 4), which is found to be more stable than the $(Al_2O_3)_{10}$ cage and $(Al_2O_3)_5-(Al_2O_3)_5$ cage-dimer. Therefore, at this size, the onion-like structure is more favorable than cage and cage-dimers. For $(Al_2O_3)_{2-9}$, it is difficult to form onion-like structures due to their small sizes.

To analyze the transformation from cage to cage-dimer to onion-like, we calculated the binding, formation, and strain energies of cage structures, and the results are shown in Figure 5 and Table 1. Since the GAUSSIAN 98 package can not be used to calculate crystal structure with the same method and same basis set as we did for $(Al_2O_3)_n$ clusters, we estimated the formation energies of $(Al_2O_3)_{1-10}$ with respect to the reactants of bulk Al and oxygen molecules using $E_f = n(E_b - 3.39 \times 2)$, where $E_b = [(2nE(Al) + 3nE(O_2/2) - E(Al_{2n}O_{3n})]/n$ and 3.39 is the experimental value for the binding energy per atom of bulk Al. From Figure 5, one can see that the binding energy increases and the strain energy decreases from $(Al_2O_3)_2$ to $(Al_2O_3)_{10}$, and the strain energies are in the range of 6.22−4.00 eV. We also note that the changes of binding energy and strain energy are very small in the size range of $5 \le n \le 10$. Therefore, considering steric and size effects, $(Al_2O_3)_5$ could be expected to have large stability, and for those clusters over $(Al_2O_3)_5$, their stabilities might be reduced. One can note from Figure 5a that, at the point where $n = 5$, there appears to be a structural transition from cage to cage-dimer. Therefore, $(Al_2O_3)_5$ can be considered to be the largest cage structure at the ground state. Furthermore, at $n = 10$, an onion-like structure is shown to be more stable than cage and cage-dimer structures by 5.22 and 2.19 eV, respectively. It may be expected to be a favorable motif for larger clusters.

Electronic properties of these different forms of aluminum oxides are now discussed. Analyzing NBO charges in $(Al_2O_3)_{1-5}$ shows that the charge transfer from the Al to the O atom is 2.2 e^-, indicating that the Al−O bond is mainly an ionic bond. We also calculated the Wiberg bond orders of Al−O bonds, which is about 0.45−0.48 for all fullerenes, suggesting that the interaction between Al and O atoms has weak covalent character in addition to ionic bond. The Mulliken population analysis shows that the Al atom carries a charge of about +1.0 e^-, and the O atom has a charge of about −0.69 e^-. As it is well-known, the charges that result from overlap populations are evenly divided into Al and O atoms in Mulliken population analyses. From the results, Al with +1.0 e^- charge and O with −0.69 e^- charge, we can see that in Al_2O_3 fullerenes Al and O atoms do not exist as Al^{3+} and O^{2-} as in bulk Al_2O_3, and there are considerable orbital overlaps between Al and O atoms. This covalent character is likely to be due to the back-donation of lone pair electrons of O to the vacant d orbitals of Al atoms.

In Table 1, we also show the adiabatic electronic affinities (EAs), $EA = E(Al_{2n}O_{3n}) - E(Al_{2n}O_{3n}^-)$, with respect to the optimized structures of both neutral and anionic clusters. The calculated small values indicate that the $(Al_2O_3)_n$ fullerenes do not easily accept an electron to transform into the corresponding anions. The shapes of the HOMOs and LUMOs of $(Al_2O_3)_{1-5}$ are shown in Figure 1. The analysis on the Kohn–Sham molecular orbitals can help us to qualitatively understand the information about chemical bonding. The HOMOs are fully occupied and dominated by oxygen 2p atomic orbitals. The LUMOs are mainly contributed from aluminum p_z atomic orbitals. For anionic clusters, the additional electrons fill in the LUMO and could be cyclic-

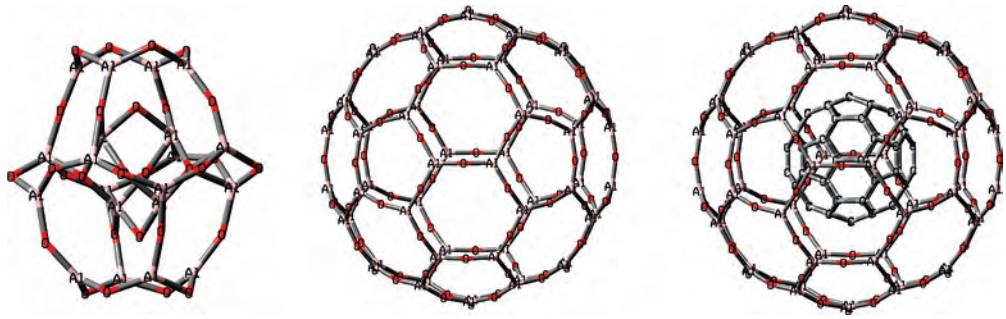

Figure 4. Optimized geometries for the $Al_4O_6@Al_{16}O_{24}$ cluster at the B3LYP/6-31G(d,p) level, and $Al_{60}O_{90}$ and $C_{60}@Al_{60}O_{90}$ at the B3LYP/6-31G(d) level.

Table 1. Symmetries, Bond Lengths (Å), Adiabatic Electron Affinities, Binding Energies, Strain Energies, and Formation Energies (eV) for $(Al_2O_3)_{1-10}$ Cages and $(Al_2O_3)_{4-10}$ Cage-Dimers at the B3LYP/6-31G(d,p) level[a]

n	group	d_{Al-O}	EA	E_b cage	E_s	E_f	E_b cage-dimer
1	D_h	1.61, 1.69	1.82	10.41	8.13	3.63	
2	C_3	1.73	2.20	15.55	6.22	17.55	
3	D_{3h}	1.72, 1.73	1.54	17.03	4.95	30.74	
4	O_h	1.71	1.99	17.61	4.26	43.33	17.24
5	C_{5h}	1.71	2.10	17.88	4.00	55.48	17.81
6	C_2	1.71	1.65	18.03	3.88	67.49	18.22
7	C_{3h}	1.70	2.07	18.13	3.81	79.46	18.24
8	S_8	1.70	2.01	18.20	3.83	91.33	18.45
9	C_s	1.70		18.25	3.81	103.24	18.53
10	C_5	1.70		18.29	3.81	115.12	18.59

[a] Binding energies are calculated by $E_b = [(2nE(Al) + 3nE(O_2/2) - E(Al_{2n}O_{3n})]/n$, and formation energies are calculated by $E_f = n(E_b - 3.39 \times 2)$, in which 3.39 is the experimental data for binding energy per atom of bulk Al.

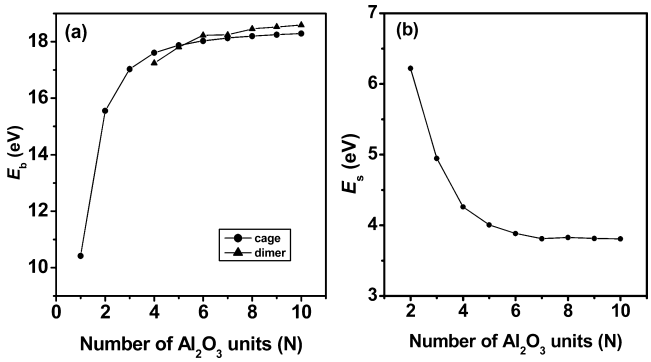

Figure 5. (a) Binding energies of cages ($1 \le n \le 10$) and cage-dimers ($4 \le n \le 10$) for $(Al_2O_3)_n$ at the B3LYP/6-31G(d,p) level. The binding energy is defined by $E_b = [(2nE(Al) + 3nE(O_2/2) - E(Al_{2n}O_{3n})]/n$. (b) Strain energies for $(Al_2O_3)_n$ ($n = 2$–10) cages at the B3LYP/6-31G(d,p) level. All strain energies were calculated from the following homodesmotic reactions suggested by George et al.;[22] i.e., $2n\ Al(OH)_3 + 3n\ Al_2O \rightarrow (Al_2O_3)_n + 6n\ AlOH$.

delocalized in forming the Al−Al σ-type orbitals, which would add to strain energy together with back-donation electrons from O lone pairs. As a result, $(Al_2O_3)_9^-$ and $(Al_2O_3)_{10}^-$ become distorted and unstable.

TEM images showed that Al_2O_3 aerosol consists of chainlike aggregates composed of small spherical primary particles.[4] $(Al_2O_3)_m + (Al_2O_3)_n \rightarrow (Al_2O_3)_m - (Al_2O_3)_n$ can be considered as a simple aggregation. Therefore, we construct $(Al_2O_3)_m-(Al_2O_3)_n$ dimers in which each cage keeps its original geometry, and the two cages can be bound by two Al−O bonds or multiple Al−O bonds. We found that the linkage with multiple bonds is more favorable than that of two Al−O bonds. The calculated binding energies between two cages are about 7 eV, suggesting that the $(Al_2O_3)_n$ cages tend to combine with each other, in good agreement with observational morphology of TEM images.[4]

With increasing cluster size, the favorable structures of $(Al_2O_3)_n$ change from cages ($n = 2-5$) to cage-dimers ($n =$ 6–9) to onion-like ones ($n \ge 10$). For large onion-like structures, $Al_{60}O_{90}$ fullerene may act as a stable shell since it is calculated to be a minimum with only real frequencies. To confirm that $Al_{60}O_{90}$ would be more stable with a core, we tried to put a C_{60} at the center of the $Al_{60}O_{90}$ cage, and the result reveals that $C_{60}@Al_{60}O_{90}$ is 0.50 eV more stable than the separated C_{60} and $Al_{60}O_{90}$ clusters. Therefore, with an appropriate core, the $Al_{60}O_{90}$ cage could be more stabilized.

B. H_2 Physisorption on $(Al_2O_3)_n$ ($n = 2$–5) Fullerenes. Hydrogen is viewed as a clean energy alternative that might one day replace fossil fuels. Alanates such as $LiAl_4$ and $Ti(AlH_4)_4$ contain more than 9 wt % hydrogen but have not been found to adsorb and release hydrogen reversibly, and the related $NaAlH_4$ material has been shown to have 5 wt % hydrogen, and hydrogen adsorption and release can take place reversibly at a temperature of 180 °C.[20]

We suggest that $(Al_2O_3)_n$ might be good candidates for hydrogen storage materials according to their cage structures and electronic characteristics. If in the $(Al_2O_3)_n$ cage each atom adsorbs one H_2 molecule, then it can reach ~9.8 wt % for hydrogen storage. In this work, the potential usage of $(Al_2O_3)_n$ for hydrogen storage was also studied.

For $(Al_2O_3)_n$ fullerenes, H_2 has five physisorption sites, that is, O top, Al top, Al−O bridge, hollow, and inside the cage. The most stable structure for H_2 adsorption we found is the site that is on the top of the surface Al atom, and the direction of H_2 is parallel to the cage surface. The next stable structure for H_2 is on the top of the surface O atom and vertical to the cage surface, and it is about 0.1−0.2 eV less stable than the H_2 adsorption on the Al atom. The most unstable adsorption site for H_2 is inside the cage; however, such instability decreases when cluster size gets bigger.

We also calculated the H_2 physisorptions on the Al_2O_3 (0001) surface with Perdew−Burke−Ernzerhof (PBE) method and plane wave (PW) basis set, included in CASTEP of Materials Studio.[24] We used an eight-layer model to simulate the Al_2O_3 (0001) surface in which the top layer is relaxed and other ones are fixed. For the Al_2O_3 (0001) surface, the

(20) Bogdanovic, B.; Schwickardi, M. *J. Alloys Compd.* **1997**, *253*, 1.

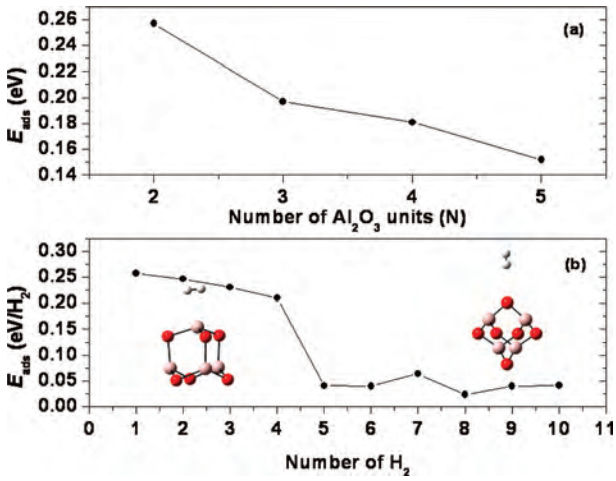

Figure 6. (a) Adsorption energies for H_2 on $(Al_2O_3)_n$ (n = 2–5) cages. (b) Adsorption energies for H_2 on Al_4O_6. The adsorption energy is defined by $E_{ads} = E(H_2) + E(Al_{2n}O_{3n}) - E(Al_{2n}O_{3n}H_2)$.

calculated H_2 adsorption energies on the O atom and Al atom are very close, and the H_2 adsorption on the O atom is slightly (0.01 eV) more stable than that on the Al atom. The calculated results suggest that the preferred sites of H_2 adsorption are different for the Al_2O_3 solid surface and the Al_2O_3 cage due to different geometrical and electronic structures.

For the most stable adsorption structure, the calculated adsorption energy of H_2 ($E_{adsorption}$) decreases with increase of cluster size as shown in Figure 6a. Obviously, the curvature can affect significantly $E_{adsorption}$. With larger fullerene sizes, the H_2−Al distance increases and tends to be a constant of 2.2 Å. From the adsorption energies ranging from 0.26 to 0.15 eV/H_2, one can see that the H_2 adsorptions on $(Al_2O_3)_n$ (n = 2–5) cages are physisorption processes, which are smaller than 0.39 and 0.65 eV/H_2 with respect to H_2 adsorptions on B- and Be-doped C_{36}.[21] In the calculations of hydrogen adsorptions, H_2 was initially located at bonding sites corresponding to chemisorptions. After relaxations, H_2 moves away from surface, and then it is stabilized at a physisorption site on these fullerenes and not dissociated. The final optimized structures with small adsorption energies correspond to physisorption stable structures.

In addition, we used Al_4O_6 as an example to study adsorption energies for various numbers of H_2. As shown in Figure 6b, the adsorption energy decreases considerably from the adsorption site at the Al atom to the O atom, whereas for equivalent adsorption sites, the adsorption energies are similar. For the H_2 adsorption on the Al atom, there is a very small Mulliken and NBO charge transfer, less than 0.05 e^-, from H_2 to Al for all fullerenes we studied. However, the electronic densities for Al_4O_6 and Al_4O_6−H_2 reveal that there is a certain accumulation of charge between H_2 and its closest Al atom (see Figure 7); that is, the presence of H_2 leads to the local deformation of the

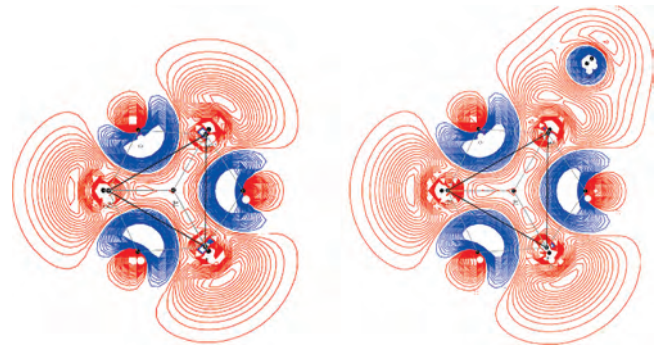

Figure 7. Electron densities for Al_4O_6 and Al_4O_6−H_2, in which electron density of the atoms is subtracted from the molecular density using the keyword BONDS in MOLDEN program.[23] The red lines correspond to negative values, blue lines to positive values. Outmost contour is 0.00125, and the contour interval is 0.00125.

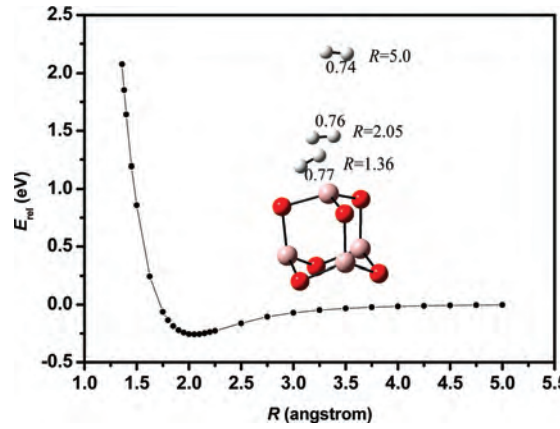

Figure 8. Relaxed potential-energy curve for the formative process of the adduct Al_4O_6−H_2 at the B3LYP/6-31G(d,p) level. R is the value of the Al−H distance. E_{rel} values are the relative energies defined by $E_{rel} = E(Al_{2n}O_{3n} - H_2) - E(H_2) - E(Al_{2n}O_{3n})$.

electron density for Al_4O_6 and thus induces a weak Coulomb interaction between H_2 and Al_4O_6.

To understand the H_2 adsorption process, we show the potential curve in Figure 8, calculated at the B3LYP/6-31G(d,p) level, for the most stable structure of $Al_4O_6(H_2)$. The calculations were performed by pointwise optimizations; that is, all geometric parameters were optimized except for the fixed Al−H bond length. It can be seen from Figure 8 that this H_2 adsorption process has no energy barrier which could significantly simplify the kinetics for the storage. Note that the formation of the Al−H bond causes the H−H bond to be weakened and the H−H bond length increases to 0.76 Å, which is about 3% longer than 0.74 Å for a free H_2 molecule. As a result, H_2 desorption can occur in a unimolecular fashion by simply overcoming the binding between H_2 and Al atoms in the fullerene. Thus, the reversible storage of H_2 in these systems appears promising.

Conclusion

Stoichiometric $(Al_2O_3)_n$ (n = 1–10 and 30) clusters were studied by using DFT calculations. The $(Al_2O_3)_{2-5}$ cages are lower in energy than other isomers and might exist under normal conditions. For $(Al_2O_3)_{6-10}$, the cage-dimer structures are shown to be more stable than the corresponding cage structures. Thus, the $(Al_2O_3)_5$ cage would be the largest cage

(21) Kim, Y.-H.; Zhao, Y. F.; Williamson, A.; Heben, M. J.; Zhang, S. B. *Phys. Rev. Lett.* **2006**, *96*, 016102.
(22) George, P.; Trachtman, M.; Bock, C. W.; Brett, A. M. *Tetrahedron* **1976**, *32*, 317.
(23) Schaftenaar, G.; Noordik, J. H. *J. Comput.-Aided Mol. Des.* **2000**, *14*, 123.

as a global minimum. For $(Al_2O_3)_{10}$, an onion-like motif has been studied, and it is found that, at this size, the onion structure is more stable than the cage and cage-dimer structures.

For larger $(Al_2O_3)_n$ clusters, onion-like structures are worthy of study. $Al_{60}O_{90}$ might act as a stable shell structure, which could be more stabilized by including a suitable core. As an example, $C_{60}@Al_{60}O_{90}$ is calculated to be 0.50 eV lower in energy than the separated C_{60} and $Al_{60}O_{90}$ cages. Searching an appropriate $(Al_2O_3)_n$ core that can most stabilize the $Al_{60}O_{90}$ cage is time-consuming and challenging. We will continue our study in this respect.

The investigation of $(Al_2O_3)_n$ cages can provide useful information to the experiments on Al combustion and oxidation. On the other hand, our calculated results show their potential uses for H_2 physisorption, suggesting that $(Al_2O_3)_n$ cages might be expected to be valuable candidates as H_2 storage materials due to their physisorption property without barriers.

Acknowledgment. This work was supported by the National Natural Science Foundation of China (Nos. 20473030, 20773047, and 60028403), and Foundation of Innovation by Jilin University.

IC7011364

(24) (a) Delley, B. *J. Chem. Phys.* **1990**, *92*, 508. (b) Delley, B. *J. Chem. Phys.* **1991**, *94*, 7245.